Systems biology informed deep learning for inferring parameters and hidden dynamics

Alireza Yazdani[1*], Maziar Raissi[1*], George Em Karniadakis[1*],

1 Division of Applied Mathematics, Brown University, Providence, RI, 02912, USA

* alireza_yazdani@brown.edu; maziar_raissi@brown.edu; george_karniadakis@brown.edu

Abstract

Mathematical models of biological reactions at the system-level lead to a large set of ordinary differential equations with many unknown parameters that need to be inferred using relatively few experimental measurements. Having a reliable and robust algorithm for parameter inference and prediction of the hidden dynamics has been one of the core subjects in systems biology, and is the focus of this study. We have developed a novel systems-biology-informed deep learning algorithm that incorporates the system of ordinary differential equations into the neural networks. Enforcing these equations effectively adds constraints to the optimization procedure that manifests itself as an imposed structure on the observational data. Using few scattered and noisy measurements, we are able to infer the dynamics of unobserved species, systematic forcing and the unknown model parameters. We have successfully tested the algorithm for three different benchmark problems.

Author summary

The dynamics of systems biological processes are usually modeled using ordinary differential equations (ODEs), which introduce various unknown parameters that need to be estimated efficiently from noisy measurements of concentration for a few species only. In this work, we present a novel "systems-informed neural network" to infer the dynamics of experimentally unobserved species as well as the unknown parameters in the system of equations. By incorporating the system of ODEs into the neural networks we effectively add constraints to the optimization algorithm, which makes the method robust to measurement noise and few scattered observations.

Introduction

Systems biology aims at a system-level understanding of biological systems, which is a holistic approach to deciphering the complexity of biological systems. To understand the biological systems, we must understand the structures of the systems (both their components and structural relationships), and their dynamics [1]. The dynamics of systems biological processes are usually modeled using ordinary differential equations (ODEs) that describe the time evolution of chemical and molecular species concentrations. Once the pathway structure of chemical reactions is known, the corresponding equations can be derived using widely accepted kinetic laws, such as the law of mass action or the Michaelis-Menten kinetics [2].

Most system-level biological models introduce various unknown parameters, which need to be estimated efficiently. Thus, the central challenge in computational modeling of these systems could be the prediction of model parameters such as rate constants or initial concentrations, and model trajectories such as time evolution of experimentally unobserved concentrations. Due to the importance of parameter estimation, a lot of attention has been given to this problem in the systems biology community. A lot of research has been conducted on the applications of several optimization techniques, such as linear and nonlinear least-squares fitting [3], genetic algorithms [4], and evolutionary computation [5]. Considerable interest has also been raised by Bayesian methods [6], which can extract information from noisy or uncertain data. The main advantage of these methods is their ability to infer the whole probability distributions of the parameters, rather than just a point estimate. More recently, parameter estimation for computational biology models has been tackled in the framework of control theory by using state observers. These algorithms were originally developed for the problem of state estimation in which one seeks to estimate the time evolution of the unobserved components of the state of a dynamical system. In this context, extended Kalman filtering [7] and unscented Kalman filtering [8] methods have been applied as well.

Due to technical limitations, however, biological reaction networks are often only partially observable. Usually, experimental data are insufficient considering the size of the model, which results in parameters that are non-identifiable [9] or only identifiable within confidence intervals. Furthermore, it is known that a large class of systems biology models display sensitivities to the parameter values that are roughly evenly distributed over many orders of magnitude. Such *sloppiness* has been suggested as a factor that makes parameter estimation difficult [10]. In the process of parameter inference, two issues accounting for system's (non-)identifiability have to be considered: *structural* identifiability that is related to the model structure independent of the experimental data [11]; and *practical* identifiability that takes into account the amount and quality of measured data. The *a priori* structural identifiability addresses the question of unique estimation of the unknown parameters based on the postulated model. However, a parameter that is structurally identifiable may still be practically non-identifiable assuming that the model is exact, but the measurements are noisy or sparse [12].

In this work, we introduce a novel systems-informed neural network to infer the *hidden* dynamics of experimentally unobserved species as well as the unknown parameters in the system of equations. By incorporating the system of ODEs into the neural networks (through adding the residuals of the equations to the loss function), we effectively add constraints to the optimization algorithm, which makes the method robust to measurement noise and few scattered observations. In addition, since large system-level biological models are typically encountered, our algorithm is computationally scalable and, hence, feasible and its output is interpretable even though it depends on a high-dimensional parameter space.

Materials and methods

Throughout this paper, we assume that the systems biological process can be modeled by a system of ordinary differential equations (ODEs) of the following form

$$\dot{\mathbf{x}} = f(\mathbf{x}, \mathbf{u}, \mathbf{p}, t), \tag{1a}$$

$$\mathbf{y} = h(\mathbf{x}) + \boldsymbol{\epsilon}(t), \quad \boldsymbol{\epsilon}(t) \sim \mathcal{N}(0, \sigma^2) \tag{1b}$$

$$\mathbf{x}(t_0) = \mathbf{x}_0, \tag{1c}$$

where the state vector $\mathbf{x}$ represents the concentration of $s = 1..S$ species, the input

signal $\mathbf{u}$ represents the external forcing and $\mathbf{p}$ is a vector of $k = 1..K$ parameters of the model, which remain to be determined. Hence, the system of ODEs f will be identified once $\mathbf{p}$ is known. The output signal $\mathbf{y}$ is the observable vector, which we can measure experimentally and could possibly be contaminated with noise $\boldsymbol{\epsilon}$ considered to be Gaussian with zero mean and standard deviation σ. The output function h is to be determined from the design of the experiments that are used for parameter inference. While h could in general be any function, it is assumed to be a linear function of the state vector $\mathbf{x}$ in most models.

Systems-informed neural networks and parameter inference

We introduce a deep learning framework that is informed by the systems biology equations that describe the kinetic pathways (Eq. (1)a) as shown in Fig. **1**. Parameters of the neural network as well as the system of equations (1) can be inferred by minimizing the following mean of squared errors loss function

$$\mathcal{L} = \text{MSE}_{data} + \alpha\ \text{MSE}_{ode} + \beta\ \text{MSE}_{aux}, \tag{2}$$

where

$$\text{MSE}_{data} = \frac{1}{NM} \sum_{m=1}^{M} \sum_{n=1}^{N} \left[y_m^n - y_m\left(t^n; \boldsymbol{\theta}, \mathbf{p}\right) \right]^2 \tag{3}$$

$$\text{MSE}_{ode} = \frac{1}{NS} \sum_{i=1}^{S} \sum_{n=1}^{N} \left[\dot{x}_i^n - f_i\left(x_i^n, \mathbf{u}^n, t^n; \boldsymbol{\theta}, \mathbf{p}\right) \right]^2, \tag{4}$$

$$\text{MSE}_{aux} = \frac{1}{S} \sum_{i=1}^{S} \left\{ \left[x_i^0 - x_i(t^0; \boldsymbol{\theta}, \mathbf{p}) \right]^2 + \left[x_i^N - x_i(t^N; \boldsymbol{\theta}, \mathbf{p}) \right]^2 \right\}. \tag{5}$$

Equation (3) is associated with the M sets of observations $\mathbf{y}_m$ given by Eq. (1)b, while Eq. (4) enforces the structure imposed by the system of ODEs given in Eq. (1)a. The parameters of the neural network $\boldsymbol{\theta}$ as well as the unknown parameters of the ODEs $\mathbf{p}$ are to be inferred. Note that observations are made on N discrete and randomly distributed time instants $t^n \in \mathcal{T}$. While the time instants used to enforce the ODEs may be chosen differently from the set of observation times, we have used the same time instants for simplicity. Additionally, the auxiliary loss function given by Eq. (5) involves two sets of data that are required by the network to pinpoint the unique dynamics of the system. The first set of data is the initial conditions at time t^0 for the state variables given by Eq. (1)c, and the second set includes the values of the state variables at any arbitrary time instant within the training time window. The final time instant t^N is considered here in this work.

Analysis of system's identifiability

A parameter p_i is identifiable if the confidence interval of its estimate $\hat{p}_i$ is finite. In systems identification problems, two different forms of identifiablity namely, *structural* and *practical* are typically encountered. Structural non-identifiability arises from a redundant parameterization in the formal solution of $\mathbf{y}$ due to insufficient mapping $\mathbf{h}$ of internal states $\mathbf{x}$ to observables $\mathbf{y}$ in Eq. (1) [9]. *A priori* structural identifiability has been studied extensively using e.g., power series expansion [13] and differential algebraic methods [14], yet mostly limited to linear models as the problem is particularly difficult for nonlinear dynamical systems. Furthermore, practical non-identifiability cannot be detected with these methods, since experimental data are disregarded.

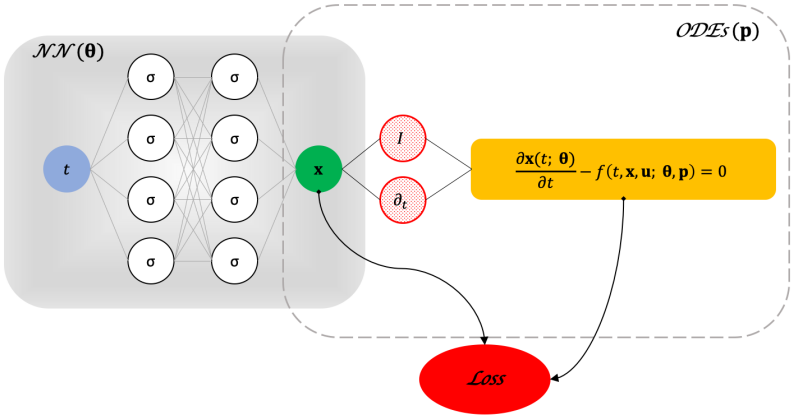

Fig. 1. *Systems biology informed deep neural networks.* An "uninformed" neural network $\mathcal{NN}(\boldsymbol{\theta})$ takes time as the input and outputs a vector of the state variables $\mathbf{x}(t;\boldsymbol{\theta})$. Scattered observations $\mathbf{y}$ are given to the network as labeled data for only a few state variables. Having an analytic representation of $\mathbf{x}(t;\boldsymbol{\theta})$, we are able to use automatic differentiation and enforce the system of equations ($ODEs(\mathbf{p})$) by adding its residuals to the loss function. This is the way to "inform" the neural networks by the governing system of ODEs.

A parameter that is structurally identifiable may still be practically non-identifiable. Practical non-identifiability is intimately related to the amount and quality of measured data and manifests in a confidence interval that is infinite. Different methods have been proposed to estimate the confidence intervals of the parameters such as local approximation of the Fisher-Information-Matrix (FIM) [12] and bootstrapping approach [15]. Another approach is to quantify the sensitivity of the systems dynamics to variations in its parameters using a probabilistic framework [16]. For identifiability analysis, we primarily use the FIM method, which is detailed in the Supporting Information.

Implementation

The algorithm is implemented in Python using the open-source Tensorflow platform [17], where the required derivatives are taken analytically using automatic differentiation. The width and depth of the neural networks depend on the size of the system of equations and the complexity of the dynamics. For the benchmark problems in this study, we have used 5-layer deep neural networks with 30 units for each state variable (e.g., for the glycolysis problem there are 7×30 units/layer). We use a standard logistic function as the activation function σ shown in Fig. 1. For the training, we use an Adam optimizer [18] with default hyper-parameters and a learning rate of 10^{-3}, where the training is performed using the full batch of data for typically 20,000 iterations. To further refine the inferred dynamics and parameters, we train the neural networks for 20,000 more iterations using a learning rate of 10^{-4}. Training was performed on a single GPU TITAN Xp, and did not take more than half hour to reach the optimal solution for the benchmark tests in this study. The source codes for these three problems are available to download at https://github.com/alirezayazdani1/SBINNs.

Results

Yeast glycolysis model

The model of oscillations in yeast glycolysis [19] has become a standard benchmark problem for systems biology inference [20, 21] as it represents complex nonlinear dynamics typical of biological systems. We use it here to study the performance of our deep learning algorithm used for parsimonious parameter inference with only two observables. The system of ODEs for this model as well as the target parameter values and the initial conditions are included in the Supporting Information. To represent experimental noise, we corrupt the observation data by a Gaussian noise with zero mean and the standard deviation of $\sigma_\epsilon = c\mu$, where μ is the mean of each observable over the observation time window and $c = 0 - 0.1$.

We start by inferring the dynamics using noiseless observations on two species $S_5 - S_6$ only. These two species are the minimum number of observables we can use to effectively infer all the parameters in the model. Figure **S1** shows the noiseless synthetically generated data by solving the system of ODEs in Eq. (4). We sample data points within the time frame of $0 - 10$ minutes at random and use them for training of the neural networks, where the neural network is informed by the the governing ODEs of the yeast model as explained above. Figure **S2** shows the inferred dynamics for all the species predicted by the systems-informed neural networks, and plotted against the exact dynamics that are generated by solving the system of ODEs. We observe excellent agreement between the inferred and exact dynamics within the training time window $0 - 10$ minutes. The neural networks learn the input data given by scattered observations (shown by symbols in Fig. **S2**) and is able to infer the dynamics of other species due to the constraints imposed by the system of ODEs.

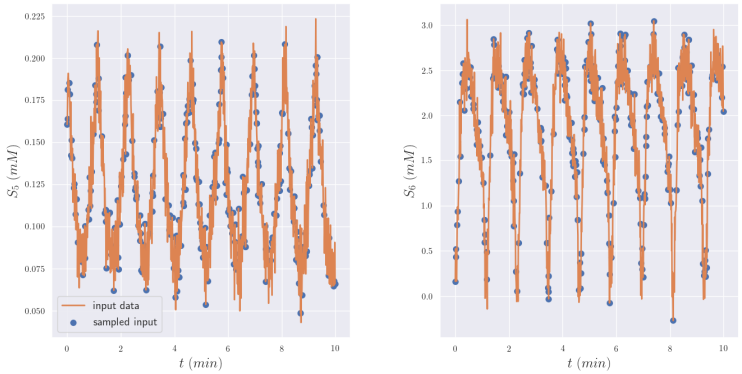

Fig. 2. *Glycolysis oscillator noisy observation data given to the algorithm for parameter inference.* Measurements are corrupted by a zero-mean Gaussian noise and standard deviation of $\sigma = 0.1\mu$. Only two observables S_5 and S_6 are considered and the data are randomly sampled in the time window of $0 - 10$ minutes.

Next, we verify the robustness of the algorithm to noise. For that purpose, we introduce Gaussian additive noise with zero mean and 10% standard deviation of the observation mean to the observational data. The input training data are shown in Fig. **2** for the same species ($S_5 - S_6$) as the observables, where similar to the previous test, we sample random scattered data points in time. Results for the inferred dynamics are shown in Fig. **3**. The agreement between the inferred and exact dynamics is excellent considering the relatively high level of noise in the training data. Interestingly, the enforced equations in the loss function in Eq. (2) act as a constraint that can effectively prevent the algorithm from overfitting the data (the noise is not overfitted as

shown in Fig. 3). The advantage of encoding the equations here is their regularization effect without using any additional L_1 or L_2 regularization.

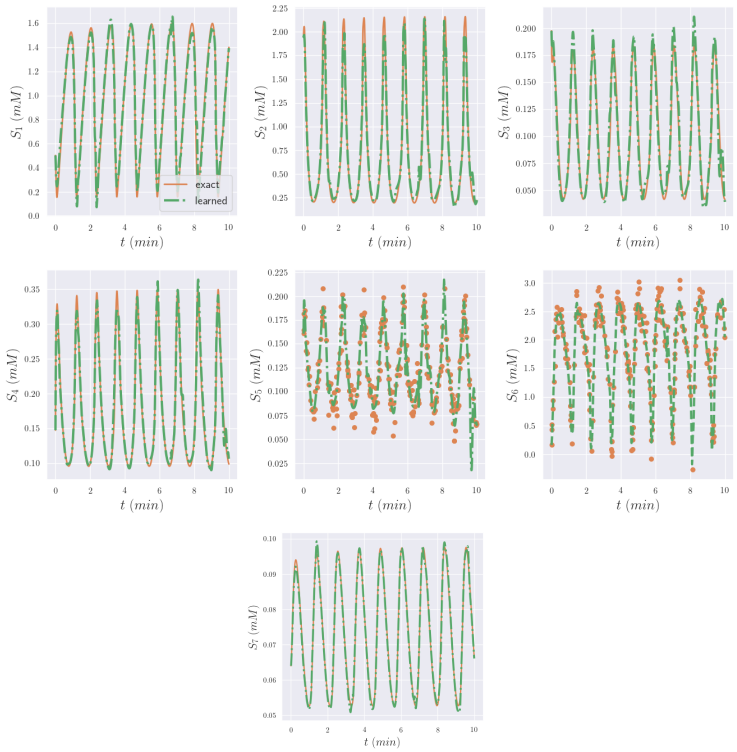

Fig. 3. *Glycolysis oscillator inferred dynamics from noisy measurements compared with the exact solution.* Predictions are performed on equally-spaced time instants in the interval of $0 - 10$ minutes. The scattered observations are plotted using symbols for the two observables S_5 and S_6. The exact data and the scattered observations are computed by solving the system of ODEs given in Eq. (4).

Table 1. Parameter values for yeast glycolysis model and each corresponding inferred values (the unit for each parameter is given in Table S1). Note that the standard deviations are estimated using Eq. (3) as practical non-identifiablity analysis based on the FIM.

Parameter	Target Value	Inferred Value (Noiseless Observations)	Inferred Value (Noisy Observations)	Standard Deviations
J_0	2.5	2.51	2.45	0.3
k_1	100	94.1	71.2	66.7
k_2	6	2.54	2.42	36.5
k_3	16	16.19	12.14	27.5
k_4	100	97.3	94.2	188.2
k_5	1.28	1.25	1.25	0.34
k_6	12	12.39	12.55	6.1
k	1.8	1.78	1.89	7.4
κ	13	13.65	13.03	50.2
q	4	4.03	3.95	0.4
K_1	0.52	0.533	0.558	0.1
ψ	0.1	0.095	0.103	0.47
N	1	2.12	2.19	5.0
A	4	3.97	4.59	3.7

Our main objective in this work, however, is to infer the unknown model parameters

p. This can simply be achieved by training the neural networks for its parameters $\boldsymbol{\theta}$ as well as the model parameters using backpropagation. The results for the inferred model parameters along with their target values are given in Table **1** for both test cases (i.e., with and without noise in the observations). First thing to note is that the parameters can be identified within a confidence interval. Estimation of the confidence intervals *a priori* is the subject of structural identifiability analysis, which is not in the scope of this work. Second, practical identifiability analysis can be performed to identify the practically non-identifiable parameters based on the quality of the measurements and the level of the noise. We have performed local sensitivity analysis by constructing the Fisher Information Matrix (FIM) using Eq. (1) and the correlation matrix $\mathbf{R}$ derived from the FIM.

The inferred parameters from both noiseless and noisy observations are in good agreement with their target values. The most significant difference can be seen for the parameters k_2 and N (close to 100% difference). However, given that the glycolysis system of Eq. (4) is identifiable (c.f. [19, 21] and Fig. **S3**), and the inferred dynamics shown in Figs. **S2** and **3** compare very well with the exact dynamics, the inferred parameters are valid. We used Eq. (3) to estimate the standard deviations of the model parameters. The σ_i estimates for the parameters are the lower bounds, and thus, may not be informative here. Further, these estimates are derived based on a local sensitivity analysis. A structural/practical identifiability analysis [9] or a bootstrapping approach to obtain the parameter confidence intervals is probably more relevant here.

Using the FIM, we are able to construct the correlation matrix $\mathbf{R}$ for the parameters. Nearly perfect correlations ($|R_{ij}| \approx 1$) suggest that the FIM is singular and the correlated parameters may not be practically identifiable. For the glycolysis model, as shown in Fig. **S3**, no perfect correlations can be found in $\mathbf{R}$ (except for the anti-diagonal elements), which suggests that the model described by Eq. (4) is practically identifiable.

Cell apoptosis model

Although the glycolysis model is highly nonlinear and difficult to learn, we have shown that its parameters can be identified. To investigate the performance of our algorithm for non-identifiable systems, we study a cell apoptosis model, which is a core sub-network of the signal transduction cascade regulating the programmed cell death-against-survival phenotypic decision [22]. The equations defining the cell apoptosis model and the values of the rate constants for the model are taken from [22] and listed in Table **S2** in the Supporting Information.

Although the model is derived using simple mass-action kinetics and its dynamics is easy to learn with our algorithm, most of the parameters are not identifiable due to both structural and practical non-identifiability. To infer the dynamics of this model, we only use random samples of measurements collected for one observable (x_4), where we assume that the measurements are corrupted by a zero-mean Gaussian noise and 5% standard deviation as shown in Fig. **4**. Furthermore, it is possible to use different initial conditions in order to produce different cell survival outcomes. The initial conditions for all the species are given in the Supporting Information, while we use $x_7(0) = 2.9 \times 10^4$ (molecules/cell) to model cell survival (see Fig. **4**(top)) and $x_7(0) = 2.9 \times 10^3$ (molecules/cell) to model cell death (see Fig. **4**(bottom)).

Using the systems-informed neural networks and the noisy input data, we are able to infer the dynamics of the system accurately as shown in Figs. **S4** and **5**. These results show excellent agreement between the inferred and exact dynamics of the cell survival/apoptosis models using one observable only.

We report the inferred parameters for the cell apoptosis model in Table **2**, where we have used noisy observations on x_4 under two scenarios of cell death and survival for comparison. The results show that only four parameters, namely $k_1, k_{d2}, k_{d4}, k_{d6}$ can be

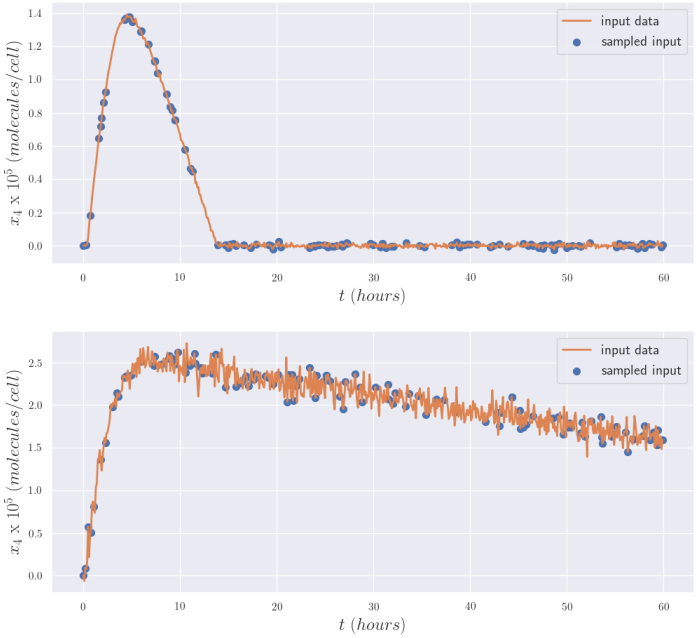

Fig. 4. *Cell apoptosis noisy observation data given to the algorithm for parameter inference.* Measurements are corrupted by a zero-mean Gaussian noise and standard deviation of $\sigma = 0.05\mu$. Data for the observable x_4 only are randomly sampled during the time window of $0 - 40$ hours for two scenarios: (top) cell survival and (bottom) cell death.

identified with relatively high accuracy using the cell survival data, while with cell death data, only two parameters k_{d2}, k_{d4} can be identified. We observe that the standard deviations for some of the parameter estimates are extremely large (e.g., for k_{d1}, k_{d3}), but are always finite. Thus, the standard deviations estimated using the FIM are not informative in practical identifiability analysis.

Table 2. Parameter values for cell apoptosis model and their corresponding inferred values (the unit for each parameter is given in Table **S2**). Note that the standard deviations are estimated using Eq. (3) as practical identifiability analysis using the Fisher Information Matrix.

		Cell Survival		Cell Death	
Parameter	**Target Value**	**Inferred Value**	**Standard Deviation**	**Inferred Value**	**Standard Deviation**
k_1	2.67×10^{-9}	0.98×10^{-9}	1.4×10^{-5}	0.25×10^{-9}	8.0×10^{-5}
k_{d1}	1×10^{-2}	1.42×10^{-4}	79.7	3.03×10^{-9}	396.6
k_{d2}	8×10^{-3}	6.29×10^{-3}	11.6	1.56×10^{-3}	107.4
k_3	6.8×10^{-8}	0.13×10^{-8}	2.7×10^{-4}	0.14×10^{-8}	8.7×10^{-4}
k_{d3}	5×10^{-2}	4.36×10^{-5}	168.0	1.6×10^{-4}	675.7
k_{d4}	1×10^{-3}	0.92×10^{-3}	0.48	0.82×10^{-3}	3.9
k_5	7×10^{-5}	1.93×10^{-7}	0.58	4.12×10^{-4}	1.3
k_{d5}	1.67×10^{-5}	6.67×10^{-11}	0.16	5.55×10^{-11}	32.1
k_{d6}	1.67×10^{-4}	1.36×10^{-4}	8.1×10^{-5}	6.05×10^{-11}	3.7×10^{-4}

To have a better picture of the practical identifiability analysis, we have plotted the correlation matrix $\mathbf{R}$ in Fig. **S5**. We observe perfect correlations $|R_{ij}| \approx 1$ between some parameters. Specifically, parameters $k_1 - k_{d1}$, and $k_3 - k_{d3}$ have correlations above 0.99 for cell survival model, which suggests that these parameters may not be

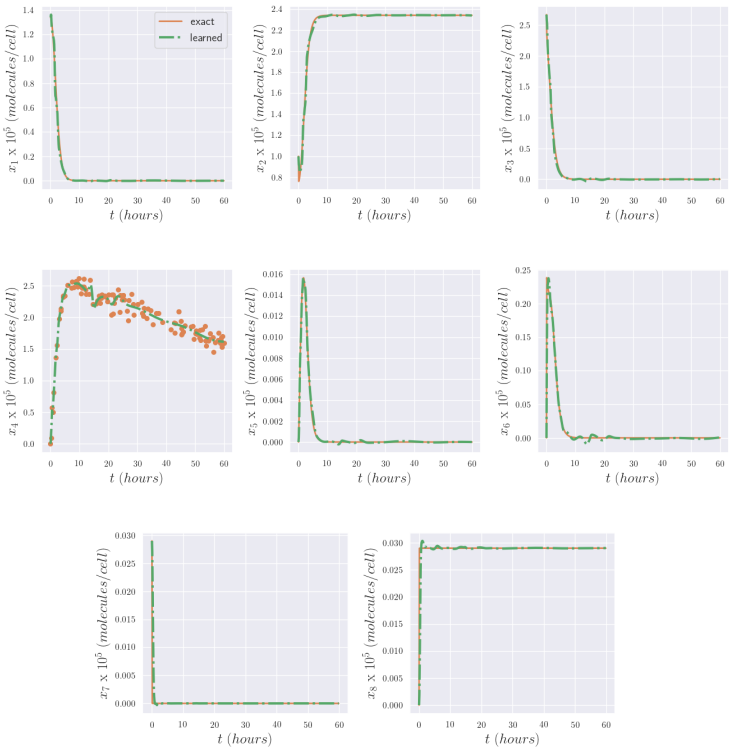

Fig. 5. *Cell apoptosis inferred dynamics from noisy observations compared with the exact solution.* Predictions are performed on equally-spaced time instants in the interval of $0 - 40$ hours. The scattered observations are plotted using symbols only for the observable x_4. The exact data and the scattered observations are computed by solving the system of ODEs given in Eq. (5).

identified. This is generally in agreement with the parameter inference results in Table **2** with some exceptions. Our parameter inference algorithm suggests that k_1 is identifiable, whereas k_{d1} is not for the cell survival model. Thus, in order to increase the power of the practical identifiability analysis and to complement the correlation matrix, we have computed the FIM null eigenvectors and for each eigenvector we identified the most dominant coefficients, which are plotted in Fig. **S6**. We observe that there are three and five null eigenvectors associated with the zero eigenvalues of the FIM for the cell survival and cell death models, respectively. The most dominant coefficient in each null eigenvector is associated with a parameter that can be considered as practically non-identifiable. These parameters include k_{d1}, k_{d3}, k_5 for the cell survival model, which agree well with the results of our algorithm. On the contrary, our algorithm suggests that parameters k_3, k_{d5} are not identifiable, whereas the above analysis has not been able to tag these parameters correctly. This could be due to the fact that they are structurally non-identifiable parameters due to issues related to the model itself such as redundancy in the equations. Similar analysis can be done for the cell death model for which our algorithm only identifies two parameters namely k_{d2}, k_{d4}.

Ultradian endocrine model

The final test case for assessing the performance of the proposed algorithm is to infer parameters of the ultradian model for glucose-insulin interaction. We use a relatively

simple ultradian model [23] with 6 state variables and 30 parameters. This is a minimal model developed in a non-pathophysiologic context and represents relatively simple physiologic mechanics.

In the ultradian model, the primary state variables are the glucose concentration G, the plasma insulin concentration I_p, and the interstitial insulin concentration I_i, which are appended with a three stage filter (h_1, h_2, h_3) that reflects the response of the plasma insulin to glucose levels [23]. The resulting system of ODEs, the nominal values for the parameters of the ultradian model along with the initial conditions for the 6 state variables are given in the Supporting Information.

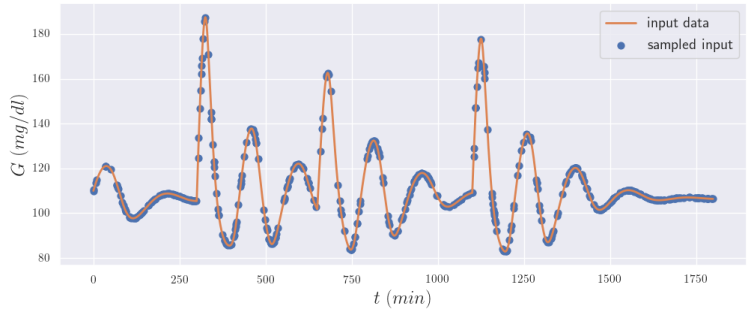

Fig. 6. *Ultradian glucose-insulin model observation data given to the algorithm for parameter inference.* Noiseless measurements on glucose level (G) only are randomly sampled in the time window of $0 - 1800$ minutes ($\sim$ one day).

The nutritional driver $I_G(t)$ is the systematic forcing of the model that represents the external sources of glucose from nutritional intake. Although the nutritional intake (modeled by the N discrete nutrition events) is required to be defined and properly recorded by the patients, it is not always accurately recorded or may contain missing values. Therefore, it would be useful to employ systems-informed neural networks to not only infer the model parameters given the nutrition events, but also to assume that the intake is unknown (hidden forcing) and infer the nutritional driver in Eq. (7)f as well.

Model parameter inference given the nutrition events

We consider an exponential decay functional form for the nutritional intake $I_G(t) = \sum_{j=1}^{N} m_j k \exp(k(t_j - t))$, where the decay constant k is the only unknown parameter and three nutrition events are given by $(t_j, m_j) = [(300, 60)\ (650, 40)\ (1100, 50)]\ (min, g)$ pairs. The only observable is the glucose level measurements shown in Fig. **6** (generated here synthetically by solving the system of ODEs), which are sampled randomly to train the neural networks for the time window of $0 - 1800$ minutes.

For the first test case, we set the parameters V_p, V_i, V_g to their nominal values and infer the rest of the parameters. The inferred values are given in Table **S4** (column Test 1), where we observe good agreement between the target and inferred values. For the second test, we infer the values of V_p, V_i, while we set $V_g = 10\ lit$. This is because one of these three volumes cannot be identified uniquely, and we choose to keep V_g fixed. Note that giving V_g a generic value will not change the inferred dynamics as other parameters will be adjusted by the algorithm to fit the observations and satisfy the equations. For example, as given in Table **S4** (column Test 2), the nominal value of the product $(C_5 V_p)$ in Eq. (7)d is 78 whereas the inferred value of this product given by the algorithm is 77.8.

Using the inferred parameters of the system of ODEs, we are able to solve the equations for unseen time instants. We perform forecasting for the second test case after training the algorithm using the glucose data in the time interval of $t = 0 - 1800\ min$ and inferring the model parameters. Next, we consider that there is a nutrition event at time $t_j = 2000\ min$ with carbohydrate intake of $m_j = 100\ g$. As shown in Fig. **S7**, we are able to forecast with high accuracy the glucose-insulin dynamics, more specifically, the glucose levels following the nutrition intake.

Model parameter inference with hidden nutrition events

As detailed in the following, one of the significant advantages of the systems-informed neural network is its ability to infer the *hidden* systematic forcing in the model. For example, in the glucose-insulin model, the nutritional driver I_G is the forcing that we aim to infer as well. Here, we use the glucose measurements to train the model for the time interval $t = 0 - 1800\ min$ shown in Fig. **6**, while we assume that the nutritional driver is additionally unknown (we include I_G in the neural networks along with the state variables). The algorithm is capable of inferring the dynamics of the model as well as the systematic forcing I_G as shown in Fig. **S8**. The neural networks have successfully inferred I_G indicating exactly when the nutrition events have occurred. However, its functional form is complex and not as easily interpretable as the original exponential decay function expressed by Eq. (7)f.

Note that the results in Fig. **S7** are produced by solving the system of ODEs given in Eq. (6) and Eq. (7), where the inferred parameters were used to reproduce the dynamics (for $t = 0 - 1800\ min$) and perform forecasting (for $t = 1800 - 3000\ min$). In Fig. **S8**, we have used the neural networks to reproduce the dynamics for the training time interval. In order to perform forecasting, we need to estimate the parameters of the nutritional intake written in the form of an exponential decay function. Using a separate optimization algorithm (we use the Nelder-Mead simplex algorithm [24]) to minimize the squared error between the exponential form of the I_G and the neural networks predictions, we are able to estimate the nutrition events pairs (t_j, m_j) and the exponential decay constant k. All the inferred parameters are given in Table **S5**.

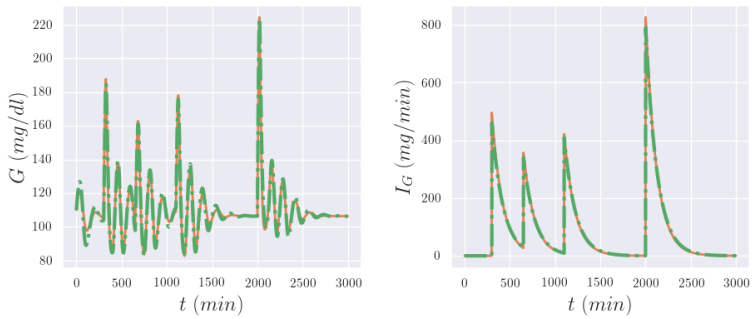

Fig. 7. *Ultradian glucose-insulin inferred dynamics and forecasting compared with the exact solution.* Predictions are performed on equally-spaced time instants in the interval of $0 - 3000$ minutes. Note that the parameter k in the intake function I_G as well as the timing (t_j) and carbohydrate content (m_j) of each nutrition event are treated as unknown and are estimated using the inferred dynamics by the neural networks for I_G. Given the inferred parameters and the exponential form of I_G, we can accurately forecast the glucose levels following the event at time $t = 2000\ min$.

Having the nutrition events as well as all other unknown parameters estimated, we

are able to solve the system of ODEs given in Eq. (6) and Eq. (7), where we are interested to forecast the glucose levels for $t = 1800 - 3000\ min$ assuming there has been a nutritional intake of $(t_j, m_j) = (2000, 100)$. The predictions for the glucose G and the nutritional driver I_G are shown in Fig. 7, which show excellent agreement in the forecasting of glucose levels.

Discussion

We presented a novel and simple to implement "systems-biology-informed" deep learning algorithm that can reliably and accurately infer the *hidden* dynamics described by a mathematical model in the form of a system of ODEs. The system of ODEs is encoded into a plain "uninformed" deep neural networks and is enforced through minimizing the loss function that includes the residuals of the ODEs. Enforcing the equations in the loss function adds additional constraints in the learning process, which leads to several advantages of the proposed algorithm: first, we are able to infer the unknown parameters of the system of ODEs once the neural network is trained; second, we can use a minimalistic amount of data on a few observables to infer the dynamics and the unknown parameters; third, the enforcement of the equations adds a regularization effect that makes the algorithm robust to noise (we have not used any other regularization technique); and lastly, the measurements can be scattered, noisy and very few. Although not pursued in this work, it is possible to separate the time instants at which the data are collected from the time instants that we enforce the residuals. Hence, we can have only few measurements and virtually an infinite number of time instants at which we enforce the equations for the minimization of the loss function.

The problem of structural and practical non-identifiability (such as the one encountered in the cell apoptosis model) is a long-standing problem in the field of systems identification, and has been under extensive research. Our goal in this work was not to propose a new identifiablity analysis method. However, we are able to use the algorithm to detect the non-identifiable parameters that can guide us to redesign the experiment, modify the model or collect additional measurements. Structural non-identifiabilities originate from incomplete observation of the internal model states. Our focus was mostly on practical identifiablity using local sensitivity analysis and the FIM. Since a structural non-identifiability is independent of the accuracy of available experimental data, it cannot be resolved by a refinement of existing measurements. One way to resolve this issue is through increasing the number of observed species.

Conclusion

We have used three benchmark problems to assess the performance of the algorithm including a highly nonlinear glycolysis model, a non-identifiable cell apoptosis model and an ultradian glucose-insulin model for glucose forecasting based on the nutritional intake. Given the system of ODEs and initial conditions of the state variables, the algorithm is capable of accurately inferring the whole dynamics with one or a few observables, where the unknown parameters are also inferred during the training process. An important and very useful outcome of the algorithm is its ability to infer the systematic forcing or driver in the model such as the nutritional intake in the glucose-insulin model.

Supporting information

S1 Fig. Glycolysis oscillator noiseless observation data given to the algorithm for parameter inference.

S2 Fig. Glycolysis oscillator inferred dynamics compared with the exact solution.

S3 Fig. Correlation matrix for the parameters of glycolysis model.

S4 Fig. Cell survival inferred dynamics from noisy observations compared with the exact solution.

S5 Fig. Correlation matrix for the parameters of the cell apoptosis model.

S6 Fig. Fisher information matrix null eigenvectors of the cell apoptosis model.

S7 Fig. Ultradian glucose-insulin inferred dynamics and forecasting compared with the exact solution.

S8 Fig. Ultradian glucose-insulin inferred dynamics with hidden nutritional driver.

S1 Table Full list of parameters for glycolytic oscillator model [19].

S2 Table Full list of parameters for cell apoptosis model [22].

S3 Table Full list of parameters for the ultradian glucose-insulin model [25].

S4 Table Parameter values for the ultradian glucose-insulin model and their corresponding inferred values (units for the parameters are given in Table S3).

S5 Table Parameter values for the ultradian glucose-insulin model and their corresponding inferred values (units for the parameters are given in Table S3).

Acknowledgments

This work was supported by the National Institutes of Health U01HL142518. Computations were supported by the National Science Foundation XSEDE resources award No. TG-DMS140007.

References

1. Kitano H. Systems biology: a brief overview. Science. 2002;295(5560):1662–1664.
2. Cornish-Bowden A, Cornish-Bowden A. Fundamentals of enzyme kinetics. vol. 510. Wiley-Blackwell Weinheim, Germany; 2012.

3. Mendes P, Kell D. Non-linear optimization of biochemical pathways: applications to metabolic engineering and parameter estimation. Bioinformatics (Oxford, England). 1998;14(10):869–883.

4. Srinivas M, Patnaik LM. Genetic algorithms: A survey. Computer. 1994;27(6):17–26.

5. Moles CG, Mendes P, Banga JR. Parameter estimation in biochemical pathways: a comparison of global optimization methods. Genome research. 2003;13(11):2467–2474.

6. Wilkinson DJ. Bayesian methods in bioinformatics and computational systems biology. Briefings in bioinformatics. 2007;8(2):109–116.

7. Lillacci G, Khammash M. Parameter estimation and model selection in computational biology. PLoS computational biology. 2010;6(3):e1000696.

8. Quach M, Brunel N, d'Alché Buc F. Estimating parameters and hidden variables in non-linear state-space models based on ODEs for biological networks inference. Bioinformatics. 2007;23(23):3209–3216.

9. Raue A, Kreutz C, Maiwald T, Bachmann J, Schilling M, Klingmüller U, et al. Structural and practical identifiability analysis of partially observed dynamical models by exploiting the profile likelihood. Bioinformatics. 2009;25(15):1923–1929.

10. Gutenkunst RN, Waterfall JJ, Casey FP, Brown KS, Myers CR, Sethna JP. Universally sloppy parameter sensitivities in systems biology models. PLoS computational biology. 2007;3(10):e189.

11. Chis OT, Banga JR, Balsa-Canto E. Structural identifiability of systems biology models: a critical comparison of methods. PloS one. 2011;6(11):e27755.

12. Rodriguez-Fernandez M, Mendes P, Banga JR. A hybrid approach for efficient and robust parameter estimation in biochemical pathways. Biosystems. 2006;83(2-3):248–265.

13. Pohjanpalo H. System identifiability based on the power series expansion of the solution. Mathematical biosciences. 1978;41(1-2):21–33.

14. Ljung L, Glad T. On global identifiability for arbitrary model parametrizations. Automatica. 1994;30(2):265–276.

15. Balsa-Canto E, Alonso AA, Banga JR. Computational procedures for optimal experimental design in biological systems. IET systems biology. 2008;2(4):163–172.

16. Foo J, Sindi S, Karniadakis GE. Multi-element probabilistic collocation for sensitivity analysis in cellular signalling networks. IET systems biology. 2009;3(4):239–254.

17. Abadi M, Agarwal A, Barham P, Brevdo E, Chen Z, Citro C, et al. Tensorflow: Large-scale machine learning on heterogeneous distributed systems. arXiv preprint arXiv:160304467. 2016;.

18. Kingma DP, Ba J. Adam: A method for stochastic optimization. arXiv preprint arXiv:14126980. 2014;.

19. Ruoff P, Christensen MK, Wolf J, Heinrich R. Temperature dependency and temperature compensation in a model of yeast glycolytic oscillations. Biophysical chemistry. 2003;106(2):179–192.

20. Schmidt M, Lipson H. Distilling free-form natural laws from experimental data. science. 2009;324(5923):81–85.

21. Daniels BC, Nemenman I. Efficient inference of parsimonious phenomenological models of cellular dynamics using S-systems and alternating regression. PloS one. 2015;10(3):e0119821.

22. Aldridge BB, Haller G, Sorger PK, Lauffenburger DA. Direct Lyapunov exponent analysis enables parametric study of transient signalling governing cell behaviour. IEE Proceedings-Systems Biology. 2006;153(6):425–432.

23. Sturis J, Polonsky KS, Mosekilde E, Van Cauter E. Computer model for mechanisms underlying ultradian oscillations of insulin and glucose. American Journal of Physiology-Endocrinology And Metabolism. 1991;260(5):E801–E809.

24. Nelder JA, Mead R. A simplex method for function minimization. The computer journal. 1965;7(4):308–313.

25. Albers DJ, Levine M, Gluckman B, Ginsberg H, Hripcsak G, Mamykina L. Personalized glucose forecasting for type 2 diabetes using data assimilation. PLoS computational biology. 2017;13(4):e1005232.